

**STRANGEONIA AND KIN; NEW RESULTS FROM
KAON HADROPRODUCTION WITH LASS***

D. ASTON,¹ N. AWAJI,² T. BIENZ,¹ F. BIRD,¹ J. D'AMORE,³
 W. DUNWOODIE,¹ R. ENDORF,³ K. FUJII,² H. HAYASHII,² S. IWATA,²
 W. B. JOHNSON,¹ R. KAJIKAWA,² P. KUNZ,¹ Y. KWON,¹ D. W. G. S. LEITH,¹
 L. LEVINSON,¹ T. MATSUI,² B. T. MEADOWS,³ A. MIYAMOTO,² M. NUSSBAUM,³
 H. OZAKI,² C. O. PAK,² B. N. RATCLIFF,^{1,◊} P. RENSING,¹ D. SCHULTZ,¹
 S. SHAPIRO,¹ T. SHIMOMURA,² P. K. SINERVO,¹ A. SUGIYAMA,² S. SUZUKI,²
 G. TARNOPOLSKY,¹ T. TAUCHI,² N. TOGE,¹ K. UKAI,⁴ A. WAITE,¹ and S. WILLIAMS¹

¹ Stanford Linear Accelerator Center, Stanford University, Stanford, CA 94305, USA

² Nagoya University, Furo-cho, Chikusa-ku, Nagoya 464, Japan

³ University of Cincinnati, Cincinnati, Ohio 45221, USA

⁴ Institute for Nuclear Study, University of Tokyo, Midori-cho, Tanashi, Tokyo 188, Japan

ABSTRACT

Recent results from a high statistics study of strangeonium mesons produced in LASS by an 11 GeV/c K^- beam are reviewed and compared with the quark model. New data from a variety of final states ($K^*\bar{K}^*$, $\phi\phi$, $\phi\pi^0$) produced by hypercharge exchange are described, and compared with results from other hadroproduction modes and from J/ψ decay.

INTRODUCTION

The nonrelativistic quark model provides a good description of most of the known light quark spectra.^{1,2)} The experimental situation is particularly well understood in the strange meson sector as has been described at this conference by David Leith.³⁾ The strangeonia are much less well understood, and a number of experiments have observed exotic candidates in final states which contain hidden strangeness and where strangonia might be expected.

This talk describes recent results on mesons with hidden strangeness from the LASS collaboration at SLAC. Details of most of these analyses in the strangeonium sector can be found elsewhere.⁴⁻⁷⁾ Results on the $K^*\bar{K}^*$, $\phi\phi$ and $\phi\pi^0$ channels are preliminary.

The spectrometer is serviced by a clean RF separated beam, and has nearly flat acceptance over 4π steradians, good particle identification, good multiparticle tracking and topology

* Work supported by Department of Energy contract DE-AC03-76SF00515; the National Science Foundation under grants No. PHY82-09144 and PHY85-13808, and the Japan-US Cooperative Research Project on High Energy Physics.

◊ Presented by B. N. Ratcliff.

*Invited talk presented at the Hadron 89: 3rd International
Conference on Hadron Spectroscopy, Ajaccio, France, September 23-27, 1989.*

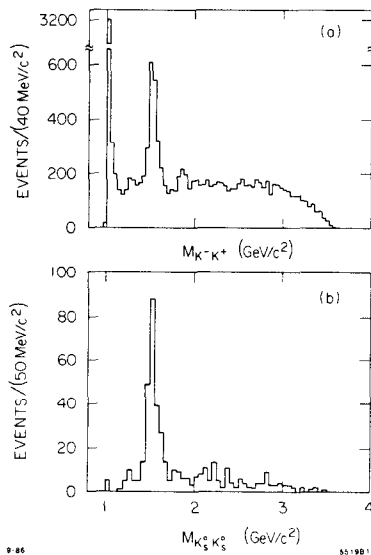


Fig. 1: The $K\bar{K}$ mass spectra from: (a) reaction (1); and (b) reaction (2).

reconstruction, a full acceptance trigger, and high data rate capability.⁸⁾ The raw data sample contains ~ 113 million triggers taken with an 11 GeV/c K^- beam, corresponding to a sensitivity of 4.1 events/nb.

$s\bar{s}$ SPECTROSCOPY

The strangeonium mesons are of particular interest since several candidates for exotic mesons couple strongly to the same final states. The reactions

$$K^- p \rightarrow K^- K^+ \Lambda \quad (1)$$

$$K^- p \rightarrow K_S^0 K_S^0 \Lambda \quad (2)$$

$$K^- p \rightarrow K_S^0 K^\pm \pi^\mp \Lambda \quad (3)$$

are dominated by peripheral hypercharge exchange which strongly favors the production of $s\bar{s}$ mesons over glueballs. Thus, these channels provide a clear look at the strangeonia, which can provide revealing comparisons with the same final states produced in other channels that might be glue-enriched. Only a very short review of the material of direct relevance to $s\bar{s}$ spectroscopy can be given here.

The mass spectrum of fig. 1(a) for reaction (1) shows bumps corresponding to the known $\phi(1020)$ and $f_2'(1525)$ leading orbital states as well as a smaller bump in the $\phi_J(1850)$ region. Only the $f_2'(1525)$ is observed in fig. 1(b) for reaction (2) since it is restricted to even spin states. In neither case is there any evidence for the $\theta(1720)$.

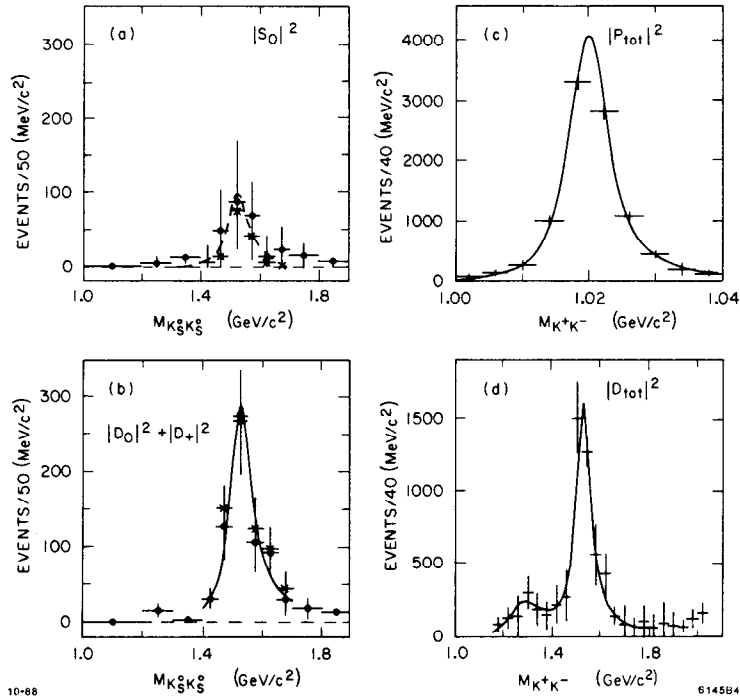


Fig. 2: The low mass $K\bar{K}$ amplitudes squared from: (a-b) reaction (2); (c-d) reaction (1).

Amplitude analyses of these data (fig. 2) display the expected P -wave structure for the $\phi(1020)$ and D -wave for the $f_2'(1525)$. In addition, the S -wave intensity [fig. 2(d)] from reaction (2) appears to peak around the $f_2'(1525)$ mass. Although the errors on the individual points are large (and nonlinear), the data require the existence of an S -wave in this region at about the 5σ level. This suggests the existence of a 0^+ resonance which is most naturally interpreted as the triplet partner of the $f_2'(1525)$,⁴⁾ and leads us to suggest that the $f_0(975)$, which is usually assigned to this multiplet, may not be a $q\bar{q}$ state.

The F -wave intensity distribution of fig. 3(a) shows a structure in the 1850 MeV/c² region which can be simply associated with the $\phi_J(1850)$ bump in the mass distribution [fig. 3(b)]. A Breit-Wigner fit to the F -wave amplitude of fig. 3(a) gives parameters $M = 1855 \pm 22$, $\Gamma = 74 \pm 67$ MeV/c², while a fit to the cross section gives $M = 1851 \pm 7$, $\Gamma = 66 \pm 29$ MeV/c². We have also shown that the interference between $s\bar{s}$ resonance production and diffractive N^* production can be utilized to analyze the leading $s\bar{s}$ amplitude, and this method gives results consistent with the above for the F -wave.⁶⁾ An extension of this method has been utilized to analyze the G -wave amplitude in the 2.2 GeV/c² mass region. Figure 4 shows evidence for a 4^+ state [the $f_4'(2210)$] which is a good candidate to be the mainly $s\bar{s}$ member of the 4^{++} nonet predicted by the quark model.

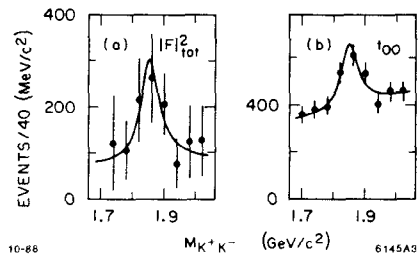


Fig. 3: The mass region around $1850 \text{ MeV}/c^2$ from reaction (1): (a) the F-wave intensity; and (b) the mass dependent total cross section.

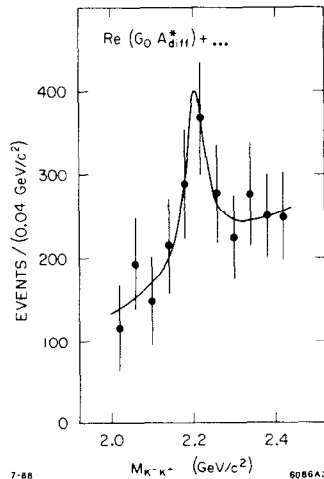


Fig. 4: The mass dependence of the interference between the G_0 and diffractive background amplitudes from reaction (1).

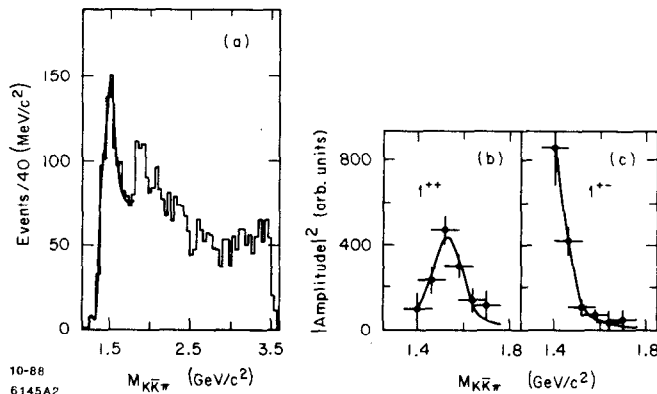


Fig. 5: The $K\bar{K}\pi$ mass distribution (a) from reaction (3); and (b-c) the 1^+ G-parity eigenstate amplitudes squared.

The most prominent features of the $K\bar{K}\pi$ mass distribution [fig. 5(a)] from reaction (3) are a sharp rise at $K\bar{K}^*(+c.c)$ threshold followed by a peak around $1.5 \text{ GeV}/c^2$, and a second peak around $1.85 \text{ GeV}/c^2$. The PWA shows that the low mass region is dominated by $1^+ K^*$ waves, while the higher mass structure contains evidence for peaks in the 2^- and 3^- waves. The 1^+ waves can be combined to form eigenstates of G-parity as shown in fig. 5(b) and 5(c). These distributions are well-described by Breit-Wigner curves as shown, and, assuming $I = 0$, provide good evidence for two $s\bar{s}$ axial-vector meson states: one with quantum numbers $J^{PC} = 1^{++}, M \sim 1530 \text{ MeV}/c^2$, and $\Gamma \sim 100 \text{ MeV}/c^2$; and the other with $J^{PC} = 1^{+-}, M \sim$

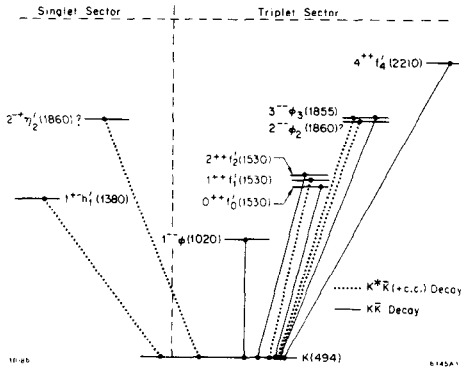


Fig. 6: Level diagram summarizing the strangeonium meson states and transitions seen in this experiment.

1380 MeV/c², and $\Gamma \sim 80$ MeV/c². These states are good candidates to be the mostly -strangeonium members of the ground state 1^{++} and 1^{+-} nonets predicted by the quark model.

Figure 6 summarizes the strangeonia observed from this experiment in the channels reviewed today. The general features of the spectrum are reminiscent of the K^* spectrum observed in LASS³⁾ although with less statistics. The observed leading states lie on an essentially linear orbital ladder that extends up through the $4^+ f_4'$, and there are good candidates for the triplet partners of the $f_2'(1525)$. Mass splittings (both $S \bullet S$ and $L \bullet S$) appear to be small. Except for the ground state pseudoscalar, the states appear to fit into SU(3) multiplets which are approximately consistent with magic mixing, and the parameters and decay transitions of these states agree well with the predictions of the quark model.^{1,9)}

OTHER STATES WITH HIDDEN STRANGENESS

Several structures have been reported recently in final states with hidden strangeness from several different production modes, and a search for production via hypercharge exchange in LASS is of interest in elucidating the nature of these effects. Preliminary analyses of the reactions

$$K^- p \rightarrow \phi \pi^0 \Lambda \quad (4)$$

$$K^- p \rightarrow \phi \phi \Lambda \quad (5)$$

$$K^- p \rightarrow K^* \bar{K}^* \Lambda \quad (6)$$

will be presented here today. The analyses of these channels and several others continue.

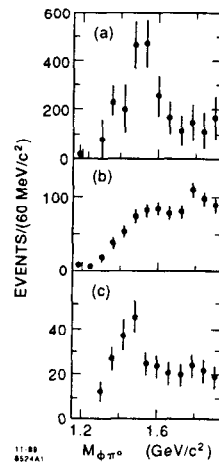


Fig. 7: The $\phi \pi^0$ mass spectrum from; (a) LEPTON-F; (b) LASS, reaction (4); and (c) LASS, reaction (4) with simulated "LEPTON-F" cuts (see text).

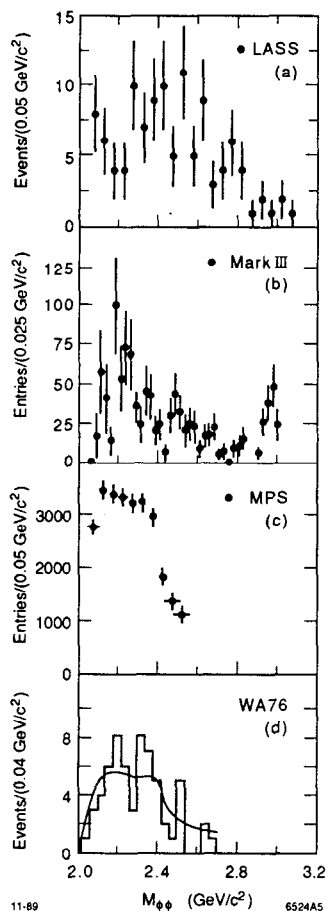


Fig. 8: The $\phi\phi$ mass spectra from: (a) reaction (5), LASS; (b) e^+e^- , radiative J/ψ decay from MARKIII; (c) π^-p , MPS spectrometer; and (d) central production in pp collisions, combined data, WA76.

different, but the apparent similarity in shape is somewhat disconcerting, and the sharp enhancement produced by simple cuts on the LASS data demonstrate how easily structures can be produced by kinematic effects.

The $\phi\phi$ system in reaction (5) has been studied in the $K^+K^-K^+K^-$ decay mode. The Dalitz plot (not shown) shows clear VV (vector-vector) $\phi\phi$ production. The invariant $\phi\phi$ mass distribution, shown in fig. 8(a), has an enhancement in the region above threshold, but this threshold structure seems to be less sharp than that produced via radiative J/ψ ,¹⁰⁾ as shown

Reaction (4) is of particular interest since the LEPTON-F group has reported a candidate for an exotic resonance in the $\phi\pi^0$ system produced by the $\pi^-p \rightarrow \phi\pi^0n$ charge exchange reaction at 32.5 GeV/c. The parameters of this object, which they call the $C(1480)$ meson, are mass = 1480 ± 80 MeV/ c^2 ; width = 130 ± 60 MeV/ c^2 ; isospin = 1; and spin-parity and charge conjugation $J^{PC} = 1^{--}$. Their observed bump at 1480 MeV/ c^2 is shown in fig. 7(a). In contrast, the $\phi\pi^0$ mass distribution from reaction (4) appears to rise slowly from threshold, as is shown in fig. 7(b), and it certainly does not peak at low mass. This is not at all surprising since the production modes and energies are different. However, an additional difference is that LASS is a 4π acceptance device whereas the LEPTON-F data are subject to a number of acceptance cuts. In particular, the energy of each photon making up the π^0 must be greater than 0.5 GeV/c; the sum of the photon energies must be greater than 5.0 GeV/c; and the charged Kaons must have momenta above 7.5 GeV/c. Therefore, it is of interest to see what effect similar cuts (scaled for energy) have on the LASS data. This simulation of the cuts can only be done approximately. In particular, the π^0 energy was required to be greater than 1.7 GeV, and the charged Kaon momenta were required to be above 2.5 GeV/c. The resulting mass distribution, shown in fig. 7(c), peaks in the low mass region, and has a bump between 1450 and 1500 MeV/ c^2 . Of course, the origins of the peaks seen in figs. 7(a) and 7(c) may be

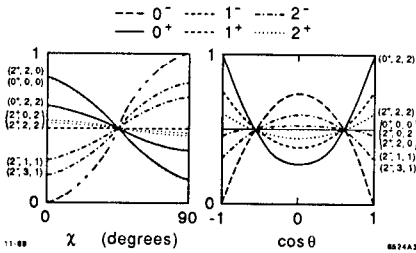


Fig. 9: The χ and $\cos\theta$ distributions for specific spin-parities of the $\phi\phi$ system (see text). They are unique only for some values of J^P . In other cases, pure (L, S) projections are shown, as labeled by (J^P, L, S).

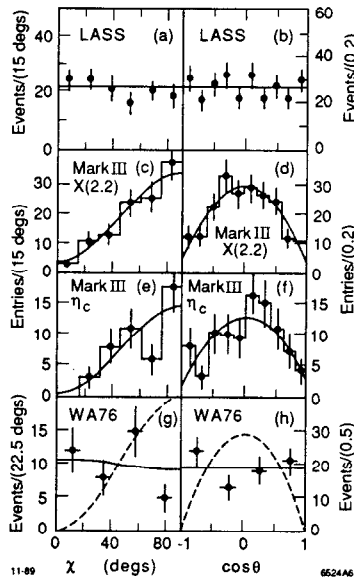


Fig. 10: The χ and $\cos\theta$ distributions for $\phi\phi$ from: (a-b) reaction (5), LASS; (c-f) radiative J/ψ decay, MARK III; (g-h) central production in pp collisions at 300 GeV/c, WA76.

in fig. 8(b). The distributions from forward π^-p collisions shown¹¹ in fig. 8(c) and central production in pp collisions¹² shown in fig. 8(d) are quite similar and appear to lie between the K^-p and e^+e^- results in terms of the sharpness of the structures.

The angular analysis of these states has been studied using the method described by Trueman,¹³ and Chang and Nelson.¹⁴ This method uses the projected distributions of two angles: the dihedral (azimuthal) angle, χ , between the vector decay planes in the VV rest frame; and the helicity (polar) angle, θ , of the K in the rest frame of the ϕ relative to the vector momentum in the VV rest frame. Examples of the expected distributions for low-spin (L, S projected) $\phi\phi$ waves¹⁰ are shown in fig. 9. Experimentally, the most important feature

of these distributions is that the 0^- wave has a distinct structure and should be observable, if dominant, while other waves, even if produced with little background, would be much harder to disentangle, particularly since for many J^P states there is more than one (L, S) combination.

The angular distributions for reaction (5) shown in figs. 10(a-b) are essentially flat. They are consistent with a pure $2^+(L, S = 0, 2)$ wave, but are also consistent with other waves or combinations of waves. However, they are clearly inconsistent with a dominant 0^- . The angular distributions seen in central production in pp collisions [figs. 10(g-h)] are also flat. In contrast, the results for the threshold $[X(2.2)]$ region from e^+e^- , figs. 10(c-d), show clear structure with negative parity, which appears to be consistent with a strong 0^- component. This is supported by its similarity to the structure observed in the η_c region which is known to be a 0^- object.

The $K^*\bar{K}^*$ system in reaction (6) has been studied both in neutral ($K^+\pi^-K^-\pi^+$) and charged ($K_S^0\pi^-K_S^0\pi^+$) decay modes. The Dalitz plots (not shown) for both reactions show clear $VV K^*(890)\bar{K}^*(890)$ production, and the background subtracted cross sections, after all corrections, are consistent with equality. As expected $\sigma_{tot}(K^*\bar{K}^*)$ is $3.6 \pm 0.3 \mu b$ for the former, and $4.0 \pm 1.1 \mu b$ for the latter charge configuration. The invariant $K^*\bar{K}^*$ mass distributions for both charge states are also quite similar, as shown in figs. 11(a) and 11(b), with a sharp enhancement

occurring in the region just above threshold. This threshold structure seems to be a consistent feature of the $K^*\bar{K}^*$ final state, essentially independent of the production mechanism. Figure 11 shows, for example, that these mass distributions are very similar to those produced via radiative¹⁰⁾ J/ψ , $\gamma\gamma$ in^{15,16)} e^+e^- , and central production in pp collisions.¹⁷⁾

The angular distributions for the $K^*\bar{K}^*$ system of reaction (6) shown in figs. 12(a-b) are essentially flat, just like the $\phi\phi$ state. They too are consistent with a pure $2^+(L, S = 0, 2)$ wave, but are also consistent with other waves or combinations of waves; however, they are inconsistent with a dominant 0^- . The angular distributions seen in central production in pp collisions (not shown) are also flat. In contrast, the results from e^+e^- , figs. 12(c-d), show

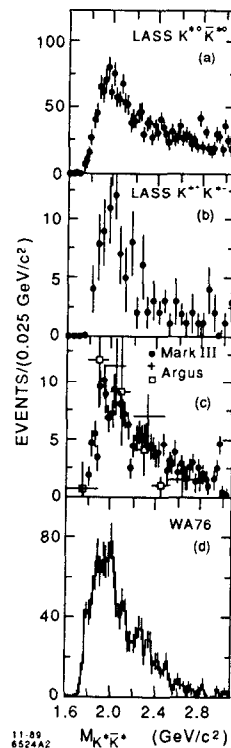


Fig. 11: The $K^*\bar{K}^*$ mass spectra from: (a) reaction (6), LASS, $K^{*0}\bar{K}^{*0}$; (b) reaction (6), LASS, $K^{*+}\bar{K}^{*+}$; (c) e^+e^- , radiative J/ψ decay from MARK III and 2γ production from ARGUS; and (d) central production in pp collisions, WA76.

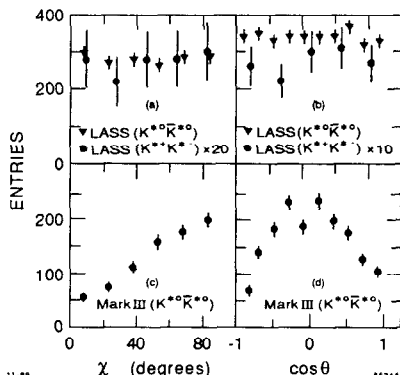


Fig. 12: The χ and $\cos\theta$ distributions for $K^*\bar{K}^*$ from: (a-b) reaction (6), LASS; and (c-d) radiative J/ψ decay, MARK III.

structure with negative parity, which appears to be consistent with a strong 0^- component. This is supported by results from a maximum likelihood ratio test which also favors a strong 0^- component.¹⁰⁾

In summary, the VV systems discussed here all show enhancements in mass near threshold. The shapes of these enhancements are quite similar, independent of production mode, for the $K^*\bar{K}^*$ systems but typically show larger differences in the $\phi\phi$ system. However, the primary differences between production modes are observed in the angular distributions. Systems produced via radiative decay from the J/ψ show strong 0^- components whereas the hadronic production modes do not. The hadronic modes are all consistent with a strong 2^+ component, but in only one case¹¹⁾ has this dominance been conclusively demonstrated. In the other channels studied to date, a combination of waves would also suffice to explain the data.

CONCLUSION

A great deal has been learned about the strangeonia in the past few years. Though confirmation is needed in several areas, in general, the $s\bar{s}$ spectrum looks remarkably similar to the strange meson system and fits expectations from the nonrelativistic quark model extremely well, as discussed above. Yet, important questions remain. With a rather clear picture of the low mass $q\bar{q}$ systems emerging, it is becoming increasingly clear that several states seen primarily in other production modes have no convenient home in the $q\bar{q}$ sector. For example, low mass 0^{++} systems have been confusing for many years, and it now seems quite clear that there are “too many” such states. The E/ι and $\theta(1720)$ regions contain many puzzles, and there are intriguing structures in the VV systems, particularly in the threshold region, which are not understood. These observations may point to the existence of meson physics beyond the quark model. We hope that the continuing analyses of data from LASS will be helpful in understanding the nature of these new spectroscopies.

REFERENCES

1. See, for example, S. Godfrey and N. Isgur, Phys. Rev. **D32** (1985) 189.
2. Particle Data Group, Phys. Lett. **170B** (1986).
3. D. Aston *et al.*, presented at this conference by D. W. G. S. Leith.
4. D. Aston *et al.* Nucl. Phys. **B301** (1989) 525.
5. D. Aston *et al.*, Phys. Lett. **201B** (1988) 573.
6. D. Aston *et al.*, Phys. Lett. **208B** (1988) 324.
7. D. Aston *et al.*, DPNU-88-24/SLAC-PUB-4661 (1988).
8. D. Aston *et al.*, The LASS Spectrometer, SLAC-REP-298 (1986).
9. S. Godfrey and N. Isgur, Phys. Lett. **141B** (1984) 439.
10. G. Eigen, presentation at this conference, CALT-68-1528 (1988), and CALT-68-1483 (revised 1987).
11. A. Etkin *et al.*, Phys. Lett. **201B** (1988) 568.
12. T. A. Armstrong *et al.*, Phys. Lett. **221B** (1989) 221.
13. T. L. Trueman, Phys. Rev. **D18** (1978) 3423.
14. N. P. Chang and C. T. Nelson, Phys. Rev. Lett. **40** (1978) 1617.
15. H. Albrecht *et al.*, Phys. Lett. **198B** (1987) 255.
16. H. Albrecht *et al.*, Phys. Lett. **212B** (1988) 528.
17. T. A. Armstrong *et al.*, CERN/EP 89-108 (1989).